Accepted Manuscript

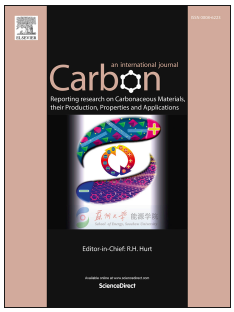

Magic auxeticity angle of graphene

Jie Hou, Binghui Deng, Hanxing Zhu, Yucheng Lan, Yunfeng Shi, Suvranu De, Li Liu, Pritam Chakraborty, Fei Gao, Qing Peng

PII: S0008-6223(19)30391-4

DOI: https://doi.org/10.1016/j.carbon.2019.04.057

Reference: CARBON 14141

To appear in: *Carbon*

Received Date: 4 December 2018

Revised Date: 26 March 2019

Accepted Date: 14 April 2019

Please cite this article as: J. Hou, B. Deng, H. Zhu, Y. Lan, Y. Shi, S. De, L. Liu, P. Chakraborty, F. Gao, Q. Peng, Magic auxeticity angle of graphene, *Carbon* (2019), doi: https://doi.org/10.1016/j.carbon.2019.04.057.

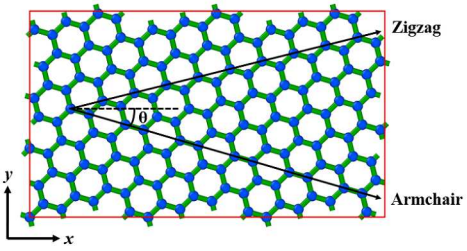

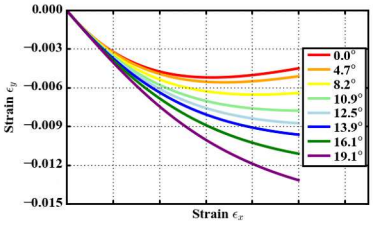

Magic Auxeticity Angle of Graphene

Jie Hou[a], Binghui Deng[b], Hanxing Zhu[c], Yucheng Lan[d], Yunfeng Shi[b], Suvranu De[a], Li Liu[a], Pritam Chakraborty[e], Fei Gao[f], Qing Peng[a,f,*]

[a]*Department of Mechanical, Aerospace and Nuclear Engineering, Rensselaer Polytechnic Institute, Troy, NY 12180, U.S.A.*
[b]*Department of Materials Science and Engineering, Rensselaer Polytechnic Institute, Troy, NY 12180, U.S.A.*
[c]*School of Engineering, Cardiff University, Cardiff CF24 3AA, United Kingdom*
[d]*Department of Physics and Engineering Physics, Morgan State University, Baltimore, MD 21251, U.S.A.*
[e]*Department of Aerospace Engineering, Indian Institute of Technology Kanpur, Kanpur, 208016, India*
[f]*Nuclear Engineering and Radiological Sciences, University of Michigan, Ann Arbor, MI 48109, U.S.A.*

Abstract

Solids exhibit transverse shrinkage when they are stretched, except auxetics that abnormally demonstrate lateral expansion instead. Graphene possesses the unique normal-auxeticity (NA) transition when it is stretched along the armchair direction but not along the zigzag direction. Here we report on the anisotropic temperature-dependent NA transitions in strained graphene using molecular dynamics simulations. The critical strain where the NA transition occurs increases with respect to an increase in the tilt angle deviating from armchair direction upon uniaxial loading. The magic angle for the NA transition is 10.9°, beyond which the critical strain is close to fracture strain. In addition, the critical strain decreases with an increasing temperature when the tilt angle is smaller than the NA magic angle. Our results shed lights on the unprecedented nonlinear dimensional response of graphene to the large mechanical loading at various temperatures.

*Corresponding author
Email address: qpeng.org@gmail.com (Qing Peng)

1. Introduction

Poisson's ratio is a mechanical parameter describing the transverse strain of materials in response to the axial deformation. Most solid materials shrink transversely when they are stretched in longitudinal direction, resulting in a positive Poisson's ratio (PPR) value. However, the abnormal ones, known as auxetics, will exhibit transverse expansion.

Graphene [1, 2], a two-dimensional sheet consisting of a monolayer carbon atoms arranged in a hexagonal lattice, is widely regarded as the wonder material in the 21st century. In recent years, many researchers have reported the intrinsic negative Poisson's ratio (NPR) in various graphene derivative materials, including not only the specifically engineered structures such as graphene ribbons [3], kirigami graphene [4], rippled graphene [5], wrinkled graphene [6, 7], porous graphene [8] and graphene-based carbon foams [9], but also the chemically altered materials such as oxidized graphene [10] and semi-fluorinated graphene [11]. Particularly, even the pristine graphene sheet could exhibit an intrinsic normal-auxeticity (NA) transition phenomenon from the normal behavior (PPR) to the auxetic behavior (NPR) under strain [3, 12]. Once the NA transition occurs, the Poissons ratio changes sign from positive to negative. This is a mechanical phase transition, belonging to second-order phase transition, which is different from thermodynamic first-order phase transition. Such unique transition exclusively occurs when the graphene reaches an engineering strain of around 6% in the armchair direction in the tensile test, while is absent in the zigzag direction. A few efforts have been devoted to explain the underlying mechanisms of such behavior in graphene. In a molecular dynamics (MD) work [12], Jiang *et al* reason out that such NA transition results from the competition between two deformation modes about the bond stretching and angle bending interaction. A recent first-principles study [13] done by Qin *et al* argues that the decentralized electron localization function driven by strain leads to the electron localization function coupling between different types of bonds, resulting in an increase of the bond angle and thus the emergence of the NPR in graphene.

Considering that the graphene, a honeycomb like structure, has a rotational symmetry in the plane and there is only 30° apart between the armchair direction and the closest zigzag direction, we hypothesize that the anisotropy of the NA transition might imply a possible critical stretching direction between the armchair and the zigzag direction with respect to this NA transition phenomenon. To explore this issue, we have carried out extensive studies by taking advantage of our previous work [14], and shown that the NA transition disappears at a magic angle θ (shown in Figure 1) of around 10.9° and this magic angle is weakly dependent on the temperature.

2. Simulation method

As well established, the method of MD simulations are widely used for various investigations [15]. Here all of our MD simulations were conducted on the platform of LAMMPS [16]. To describe the inter-atomic force among carbon atoms, we adopted the adaptive intermolecular reactive empirical bond order (AIREBO) potential [17], which has been widely utilized to investigate the mechanical properties of the carbon systems. A well known issue about the AIREBO potential is the artificial strengthening before failure [18, 19, 20], characterized as a sharp upward angle just before the drop in a stress-stress curve. It turns out that this artificial strengthening is caused by its cutoff distances (r_{cc}^{min} and r_{cc}^{max}) in its switching function defining the C−C interaction between r_{cc}^{min} and r_{cc}^{max}, which is in the format of:

$$f(r) = \begin{cases} 1, & r < r_{cc}^{min} \\ \frac{1}{2}[1 + \cos(\frac{r - r_{cc}^{min}}{r_{cc}^{max} - r_{cc}^{min}})], & r_{cc}^{min} \leqslant r \leqslant r_{cc}^{max} \\ 0, & r > r_{cc}^{max} \end{cases} \tag{1}$$

The original type of AIREBO potential has $r_{cc}^{min} = 1.7$ Å and $r_{cc}^{max} = 2.0$ Å. Those cutoff values model the carbon covalent bond well at the vicinity of its equilibrium distance. However, when the system is stretched to a certain amount beyond 0.1 of strain, the C-C distances fall into the switching region, bringing in an artificial strengthening of C−C bonds. To adopt the AIREBO potential for large deformation, researchers generally modify the cutoff distances according to the specific systems studied [18, 19, 20]. We have examined this r_{cc}^{min} parameter and adopted the value of 1.92Å, as reported in our previous work[14]. The stress-strain curves are extremely insensitive to the cutoff distances under the strain below 0.1. The influence of the cutoff values becomes non-negligible in the regime of the strain above 0.1. We adopt the same cutoff values $r_{cc}^{min} = 1.92$ Å and report our results under the strain from 0 to 0.1 only.

The structure of monolayer graphene was built up in the way that the tilted two-dimensional layer would lie in the x-y plane. The tilt angle θ, away from the armchair direction as shown in Figure 1, defined the stretching direction in the tensile test. Due to the six-fold symmetry, the tilt angle is continuously ranged from 0° to 30°. However, since we expect to apply the periodic boundary condition on both the x and y directions to eliminate the edge effect, the tilt angle must be carefully chosen due to the restriction of the atomistic structure. As a result, we selected eight monolayer graphene samples with θ

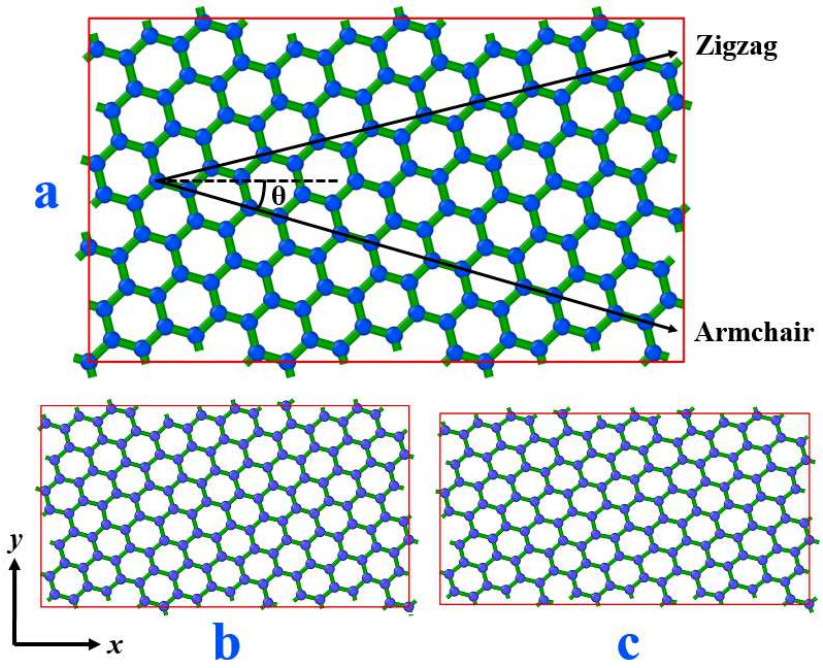

Figure 1: (a) A schematic plot of tilted monolayer graphene layout in the x-y plane with tilt angle $\theta = 16.1°$. Periodic boundary conditions are applied in in-plane directions.(b)(c) The snapshot of the deformed sample at the strain of 0.05 and 0.10 separately.

of 0.0°, 4.7°, 8.2°, 10.9°, 12.5°, 13.9°, 16.1°and 19.1° respectively. Each sample has a similar size of about 200Å×200Å and consists of about 16,000 carbon atoms. These configurations are selected to ensure that the system size has trivial effects on the results [21]. Details about the graphene samples are summarized in Table 1 of the supplementary materials.

For all the simulations, the time step was set at 0.00025 ps and the Newton's equation of motion were numerically integrated using the velocity-Verlet algorithm [22]. In each tensile test, the graphene sample was initially relaxed for 20 ps at the specific temperature and zero external pressure using the isothermal-isobaric ensemble dynamics to reach the equilibrium. Subsequently, the sample was still kept relaxed in the y direction, but got subjected to a uniaxial tensile test along the x direction with an engineering strain rate of 10^9 s^{-1}. The sizes of the sample in both the x and y directions were calculated and output every 1,000 steps by taking the mean values at 600 consecutive steps respectively. The temperature and pressure were controlled by the Nose-Hoover thermostat and barostat [23, 24]. The boundary conditions were periodic in both the x and y direction but fixed in the z direction. The OVITO software [25] was used to realize visualization and generate snapshots.

3. Results and discussion

We have examined the collateral strain and Poisson's ratio as a function of the tensile strain in eight graphene samples. The engineering strain in the y direction is defined as $\epsilon_y = (L_y - L_{y0})/L_{y0}$, where L_{y0} and L_y are the lengths of sample in the y direction before and after the deformation. Similarly, the strain in the x direction is defined as $\epsilon_x = (L_x - L_{x0})/L_{x0}$, where L_{x0} and L_x are the lengths of sample in the x direction before and after the deformation. The collateral strain evolutions at the temperature of 300K are shown in Figure 2(a), where the data are obtained by fitting the $\epsilon_x - \epsilon_y$ curves into 4th order polynomial functions.

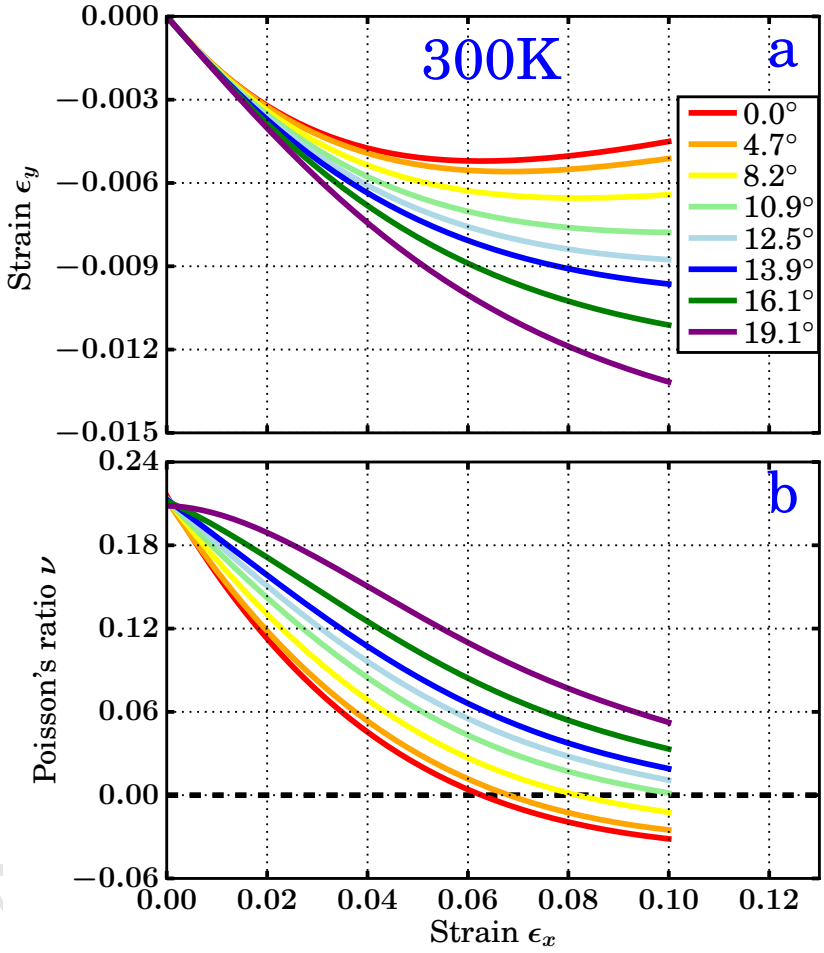

Figure 2: Dependence of the NA transition on the stretching direction in the monolayer graphene at 300K. (a) The engineering strain ϵ_y vs ϵ_x at θ ranging from 0.0° to 19.1°. (b) Corresponding Poisson's ratio ν in the monolayer graphene at different θ.

Figure 2(b) illustrates the accompanying evolutions of Poisson's ratio ν for the uniaxial

tensile test in the x direction at the temperature of 300K. Here the Poisson's ratio is defined as [26] $\nu = -d\epsilon_y/d\epsilon_x$. There are two ways to define the Poisson's ratio, depending on the amount of the deformations. Analog to the two definitions of strain, *engineering* strain and *true* strain, we could denote the two definitions as *engineering* Poisson's ratio ($\nu = -\epsilon_y/\epsilon_x$) and *true* Poisson's ratio ($\nu = -d\epsilon_y/d\epsilon_x$). The *engineering* Poisson's ratio is good for *small* deformation, and the *true* Poisson's ratio is good for *large* deformation beyond linear elastic strain region. The Poisson's ratio we used here is the true Poisson's ratio due to the large deformation we applied in this study. To avoid confusing, the Poisson's ratio are all true Poisson's ratio in this study except special notice.

The NA transition occurs when ν changes from positive (normal) to negative (auxetic). The corresponding strain is named as the critical strain of the NA transition. When the tilt angle θ is smaller than 10.9°, graphene will take the transition from PPR to NPR before ϵ_x reaches 0.1. For the tilt angle θ larger than 10.9°, no NA transition phenomena are observed in the range of ϵ_x from 0 to 0.1. In other words, 10.9° is the critical angle where the NA transition phenomenon of graphene will occur at a strain ϵ_x no higher than 0.1 at the room temperature. In addition, the critical strain increases with respect to an increase of tilt angle θ (Figure 2(b)).

We also explored the effect of temperature on the NA transition behavior of the monolayer graphene at different θ. The tensile tests at different temperatures (600K, 900K, 1200K and 1500K) were further conducted on the graphene samples. Figure 3 shows the dependence of the NA transition behavior on the stretching direction for the monolayer graphene at 1500K. Similar dependences at other temperatures are shown in the supplementary materials. Figure 3 illustrates that the NA transition occurs in the monolayer graphene when θ is 10.9°, but disappears when θ is 12.5° in the range of ϵ_x from 0 to 0.1, suggesting that the magic angle where the NA transition phenomenon occurs is slightly higher than 10.9° but lower than 12.5° at 1500K. As it has been shown in the supplementary materials, at other temperatures from 600K to 1200K, the magic angle also lies between 10.9° and 12.5°, suggesting its insensitivity to the temperature.

It is worth noting that though it has been theoretically predicted that the NPR at the zero strain is isotropic with six-fold fold-rotation symmetric structures at zero temperature [27], we observe that the Poisson's ratio results with different θ do not completely converge at $\epsilon_x = 0$ at the finite temperatures. MD studies [28, 29] show that the value of Young's modulus obtained by linearly fitting the stress-strain curve near the zero strain with the AIREBO force-field slightly varies along the armchair and zigzag directions. A more detailed study

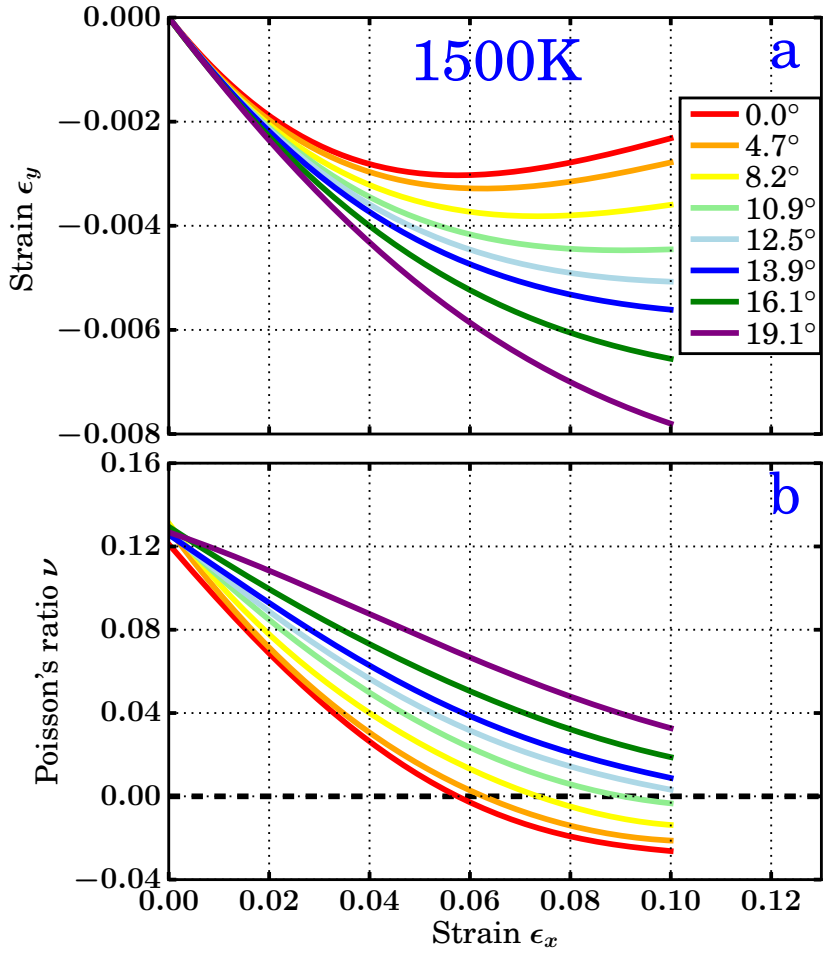

Figure 3: Dependence of the NA transition on the stretching direction in the monolayer graphene at 1500K. (a) The engineering strain ϵ_y vs ϵ_x at θ ranging from 0.0° to 19.1°. (b) Corresponding Poisson's ratio ν of the monolayer graphene at different θ.

[21] even demonstrates that the Young's modulus value of graphene, calculated with the AIREBO force-field, monotonically decreases from along the armchair direction to along the zigzag direction. Such a non-isotropic mechanics might attribute to the nonlinear elasticity at finite temperatures.

The critical strain of the NA transition in the monolayer graphene strongly depends on the tilt angle θ and temperature, as illustrated in Figure 4. As a general trend, the critical strain decreases with the increasing temperature when θ is fixed, but increases with the increasing θ when the temperature is fixed. In addition, when the temperature is fixed, the critical strain changes more swiftly in response to an increase of θ at larger θ, suggesting that it is more sensitive to larger θ. Moreover, the critical strain has a higher decreasing rate at higher θ in response to the increasing temperature.

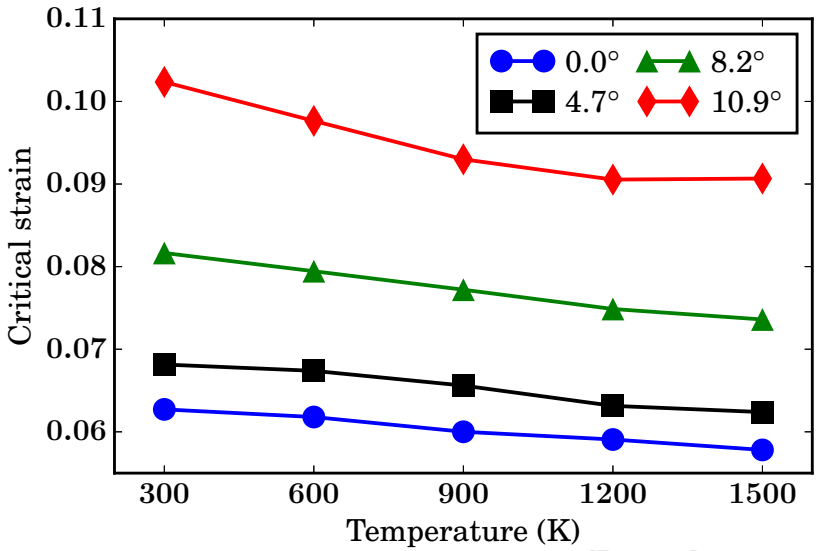

Figure 4: Dependence of the critical strain of the NA transition on the tilt angle and temperature in the monolayer graphene.

The auxetic materials have great potential for wide applications, such as protective structures [30] (e.g. body armor and shock absorber), novel biomedical structures [31] (e.g. artificial blood vessels, ligament anchors), and traditional mechanical components [32] (e.g. aero engine blades and wing panels). However, most auxetic materials and structures generally have a substantial porosity in their geometrical configuration, naturally demoting their mechanical performance at the very beginning [33]. Generally, such sacrifices cannot be compensated by the obtained auxetic behavior and therefore limits the practical application of the auxetics. Fortunately, graphene is immune from such weakness since it has a tensile modulus of 1 TPa [34], adding itself to the list of the strongest and stiffest materials ever tested. Combined with its biocompatibility [31] and its insensitivity of the NA transition to the surrounding temperature, graphene has considerable applications in the aspect of auxeticity in a wide temperature span.

4. Conclusion

In summary, we have investigated the anisotropic and temperature-dependent auxetic behaviors of the monolayer graphene using the molecular dynamics simulations. We have explicitly examined eight configurations with the tilt angle ranging from 0° to 19.1° with respect to the armchair direction. We have found the magic angle of 10.9°, and beyond which the NA mechanical transition disappears in the range of strain from 0 to 0.1. Further molecular dynamics studies have revealed that this NA magic angle slightly increases (by

less than 1.6°) when the temperature increases from 300 K to 1500 K. This study might be helpful in understanding nonlinear mechanics of graphene and exploring its potential applications.

Acknowledgement

The authors would like to acknowledge the generous financial support from Battelle Energy Alliance, LLC under the DOE Idaho Operations Contract DE-AC07-05ID14517.

Disclosure statement

Authors have no conflict of interest to declare.

References

[1] Novoselov K, Geim A, Morozov S, Jiang D, Zhang Y, Dubonos S, et al. Electric field effect in atomically thin carbon films. Science. 2004;306(5696):666–669.

[2] Novoselov K, Geim A, Morozov S, Jiang D, Katsnelson M, Grigorieva I, et al. Two-dimensional gas of massless Dirac fermions in graphene. Nature. 2005;438(7065):197–200.

[3] Jiang JW, Park HS. Negative Poisson's Ratio in Single-Layer Graphene Ribbons. Nano Lett. 2016;16(4):2657–2662.

[4] Cai K, Luo J, Ling Y, Wan J, Qin Qh. Effects of size and surface on the auxetic behaviour of monolayer graphene kirigami. Sci Rep. 2016;6(35157).

[5] Qin H, Sun Y, Liu JZ, Li M, Liu Y. Negative Poisson's ratio in rippled graphene. Nanoscale. 2017;9(12):4135–4142.

[6] Grima JN, Winczewski S, Mizzi L, Grech MC, Cauchi R, Gatt R, et al. Tailoring Graphene to Achieve Negative Poisson's Ratio Properties. Adv Mater. 2015;27(8):1455–1459.

[7] Grima JN, Grech MC, Grima-Cornish JN, Gatt R, Attard D. Giant Auxetic Behaviour in Engineered Graphene. Ann Phys (Berl). 2018;530(6).

[8] Ho VH, Ho DT, Kwon SY, Kim SY. Negative Poisson's ratio in periodic porous graphene structures. Phys Status Solidi B. 2016;253(7):1303–1309.

[9] Zhang J, Xiong Q. The negative Poisson's ratio in graphene-based carbon foams. Phys Chem Chem Phys. 2018;20(6):4597–4605.

[10] Wan J, Jiang JW, Park HS. Negative Poisson's ratio in graphene oxide. Nanoscale. 2017;9(11):4007–4012.

[11] Qin R, Zheng J, Zhu W. Sign-tunable Poisson's ratio in semi-fluorinated graphene. Nanoscale. 2017;9(1):128–133.

[12] Jiang JW, Chang T, Guo X, Park HS. Intrinsic Negative Poisson's Ratio for Single-Layer Graphene. Nano Lett. 2016;16(8):5286–5290.

[13] Qin Z, Qin G, Hu M. Origin of anisotropic negative Poisson's ratio in graphene. Nanoscale. 2018;10(22):10365–10370.

[14] Deng B, Hou J, Zhu H, Liu S, Liu E, Shi Y, et al. The normal-auxeticity mechanical phase transition in graphene. 2D Materials. 2017;4(2):021020.

[15] Peng Q, Meng F, Yang Y, Lu C, Deng H, Wang L, et al. Shockwave generates < 100 > dislocation loops in bcc iron. Nat Commun. 2018;9:4880.

[16] Plimpton S. Fast parallel algorithms for short-range molecular-dynamics. J Comput Phys. 1995;117(1):1–19.

[17] Stuart S, Tutein A, Harrison J. A reactive potential for hydrocarbons with intermolecular interactions. J Chem Phys. 2000;112(14):6472–6486.

[18] Huhtala M, Krasheninnikov A, Aittoniemi J, Stuart S, Nordlund K, Kaski K. Improved mechanical load transfer between shells of multiwalled carbon nanotubes. Phys Rev B. 2004;70(4).

[19] Wei Y, Wu J, Yin H, Shi X, Yang R, Dresselhaus M. The nature of strength enhancement and weakening by pentagon-heptagon defects in graphene. Nat Mater. 2012;11(9):759–763.

[20] Grantab R, Shenoy VB, Ruoff RS. Anomalous Strength Characteristics of Tilt Grain Boundaries in Graphene. Science. 2010;330(6006):946–948.

[21] Hossain MZ, Hao T, Silverman B. Stillinger-Weber potential for elastic and fracture properties in graphene and carbon nanotubes. J Phys Condens Matter. 2018;30(5).

[22] Binder K, Horbach J, Kob W, Paul W, Varnik F. Molecular dynamics simulations. J Phys Condens Matter. 2004;16(5, SI):S429–S453. Euroschool on New Materials and their Dynamics - Advances Through Synchrotron Radiation, Rostock Warnemunde, GERMANY, SEP 29-OCT 11, 2002.

[23] Nose S. A unified formulation of the constant temperature molecular-dynamics methods. J Chem Phys. 1984;81(1):511–519.

[24] Hoover W. Canonical dynamics - Equilibrium phase-space distributions. Phys Rev A. 1985;31(3):1695–1697.

[25] Stukowski A. Visualization and analysis of atomistic simulation data with OVITO-the Open Visualization Tool. Model Simul Mater Sci Eng. 2010;18(1):015012.

[26] Ho DT, Park SD, Kwon SY, Park K, Kim SY. Negative Poisson's ratios in metal nanoplates. Nat Commun. 2014;5(3255).

[27] Thomas S, Ajith KM, Valsakumar MC. Directional anisotropy, finite size effect and elastic properties of hexagonal boron nitride. J Phys Condens Matter. 2016;28(29):295302.

[28] Li M, Deng T, Zheng B, Zhang Y, Liao Y, Zhou H. Effect of Defects on the Mechanical and Thermal Properties of Graphene. Nanomaterials. 2019;9(3).

[29] Pei QX, Zhang YW, Shenoy VB. A molecular dynamics study of the mechanical properties of hydrogen functionalized graphene. Carbon. 2010 MAR;48(3):898–904.

[30] Sun Y, Pugno N. Hierarchical Fibers with a Negative Poisson's Ratio for Tougher Composites. Materials. 2013;6(2):699–712.

[31] Pinto AM, Goncalves IC, Magalhaes FD. Graphene-based materials biocompatibility: A review. Colloids Surf B. 2013;111:188–202.

[32] Saxena KK, Das R, Calius EP. Three Decades of Auxetics Research - Materials with Negative Poisson's Ratio: A Review. Adv Eng Mater. 2016;18(11):1847–1870.

[33] Ren X, Das R, Tran P, Ngo TD, Xie YM. Auxetic metamaterials and structures: a review. Smart Mater Struct. 2018;27(2):023001.

[34] Lee C, Wei X, Kysar JW, Hone J. Measurement of the elastic properties and intrinsic strength of monolayer graphene. Science. 2008;321(5887):385–388.